# **ESI:** Design and Fabrication of a Novel On-Chip Pressure Sensor for Microchannels

Nishagar Raventhiran, Razin Sazzad Molla, Kshithij Nandishwara, Erick Johnson and Yaofa Li

*Mechanical & Industrial Engineering Department, Montana State University*

---

**Abstract**

This PDF includes:

- Text on calibration setup
- Text on cross-section measurement
- Text on numerical simulation execution
- Tex on calibration repeatability test
- Figures S1–S5
- Table I

---

## 1. Generation of Constant Pressure Head

The pressure calibration was intended to capture the shapes of fluorescent particle images at various prescribed pressures. The pressure was controlled by a water tank which sustains hydrostatic pressure as shown in Figure 1. By raising or lowering the height of the water tank, the pressure can be changed according to the hydrostatic pressure equation of,

$$p = \rho g(H - h) \tag{1}$$

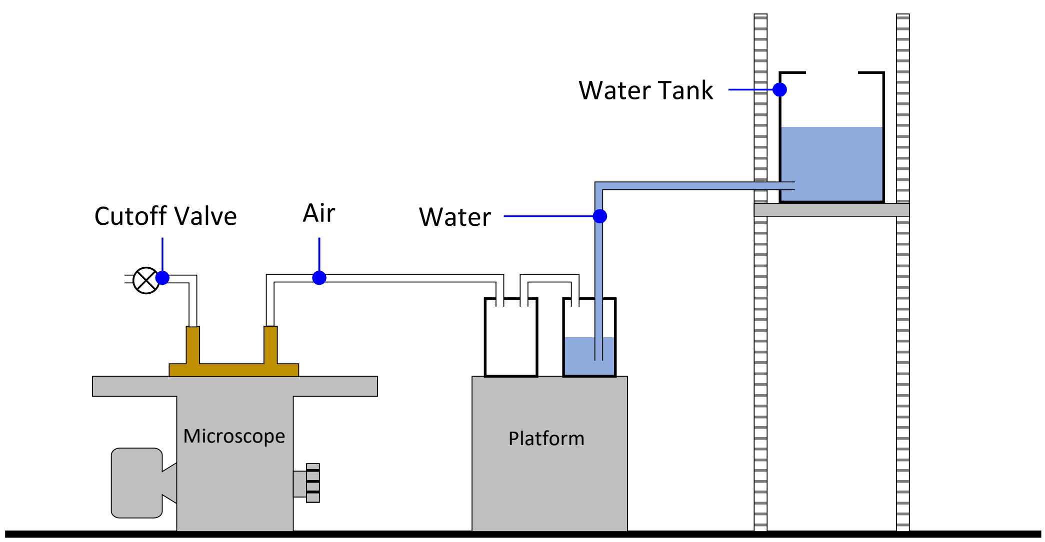


Figure S1: A schematic diagram of the setup used for pressure calibration.

where $p$ is the hydrostatic pressure, $\rho$ is the density of the driving fluid, $g$ is the gravitational acceleration, $H$ is the height of the water level in the tank relative to the optical table and $h$ is the height of the water in the glass bottle again relative to the optical table. The water tank and the glass bottle on the right both contains water and the level difference between them creates the net hydrostatic pressure. Here the hydrostatic pressure generated by the air in the tubing is neglected due to its much smaller density. A second glass bottle was used as a buffer chamber to separate from the driving fluid the microchannel to avoid any potential contamination. The pressure calibration was started at zero pressure difference by lowering the tank to the same level of the glass bottle. The pressure was then increased gradually by raising the tank at an increment of 1 cm.

## 2. Characterization of the Microchannel Cross-Section

It is well known that PDMS microchannels fabricated using soft lithography often do no have perfectly square or rectangular cross-sections due to the flexible nature of PDMS and other fabrication errors. To ensure accurate calculation of numerical and theoretical values for validation purpose, the microchannels used in this study were characterized using an optical profilometer (Profilm3D). Additionally, the cross-section was also directly imaged using a microscope (Olympus IX71) by cutting the microchannel at various locations in the perpendicular direction. Combining the two types of measurements, the actual cross-sectional shape was determined. As shown in Figure 2, the cross-section shape is largely trapezoidal, with curved edges and rounded corners. The height of the microchannel is $\sim$123 $\mu$m. While the top of the microchannel is $\sim$112 $\mu$m wide, the bottom is only $\sim$96 $\mu$m wide. This complex geometry of the cross-section coupled with the U-shape design of the microchannel necessities the use of numerical method to determined the expected values of pressure drop as detailed below.

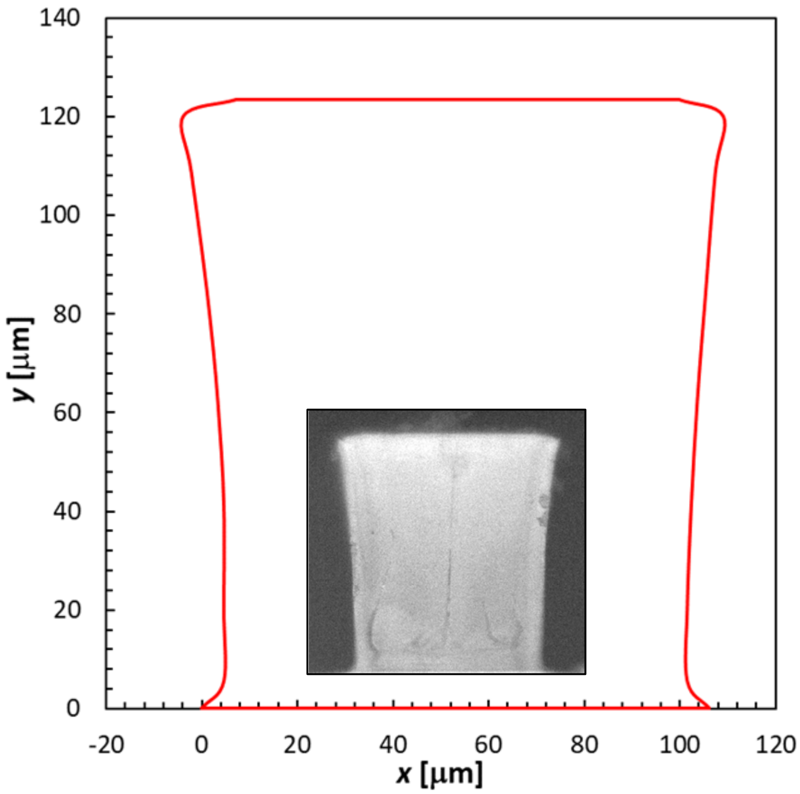


Figure S2: The actual shape of the microchannel cross-section. The inset shows a micro-scope photo of the cross-section.

## 3. Numerical Simulation in Star-CCM+

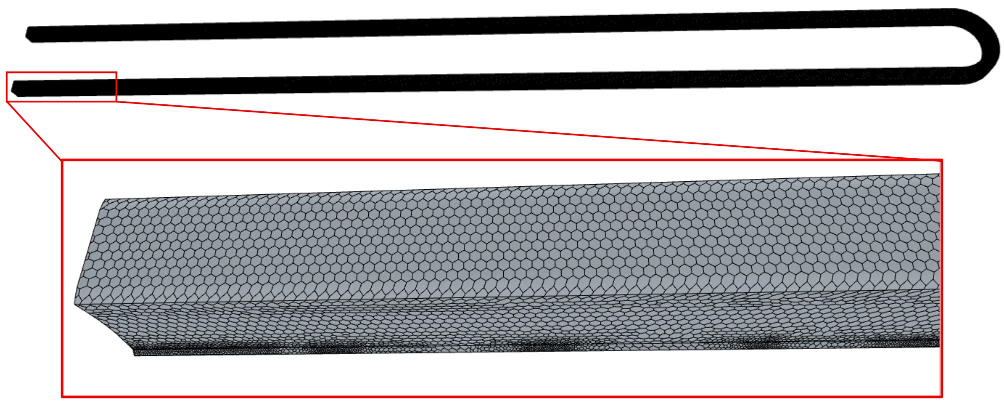

Figure S3: The meshed geometry illustrating the polyhedral meshes.

To validate our experimental measurement, the expected pressure drop in the microchannel was numerically solved in Star-CCM+ (v16.04.007). The 3D geometry of the microchannel was based on the original photomask design, reproducing the cross-section characterization in SolidWorks before being imported into Star-CCM+. A polyhedral mesh was generated with an average element size of $10\,\mu$m, resulting a total of 1,121,931 elements. It is worth noting that the base size was selected after a mesh sensitivity analysis was completed at the largest Reynolds number to ensure the wall shear stress was appropriately captured. Figure 3 shows a snapshot of the meshed geometry. Given the extremely low Reynolds numbers, the flow was assumed to be incompressible and laminar, with water properties at 23°C (*i.e.*, the measured lab temperature when the experiments were performed). The physical properties of water and air at 23°C are listed in Table 1. A uniform velocity inlet is derived from the desired mass-flow rate and the outlet is a pressure boundary condition set to 0 kPa (gauge). The walls are considered no-slip. Figure 5 shows a sample pressure field within the microchannel for single-phase flow of air at 1 ml/min. As expected, the pressure gradually decreases from the inlet to the outlet. The pressure drop between inlet and outlet at this condition is 1.02 kPa.

Table 1: Physical properties of water and air at 23°C.

| $\rho_{\text{water}}$ [kg/m$^3$] | $\rho_{\text{air}}$ [kg/m$^3$] | $\mu_{\text{water}}$ [Pa·s] | $\mu_{\text{air}}$ [Pa·s] |
|---|---|---|---|
| 997.5 | 1.192 | $9.35 \times 10^{-4}$ | $1.83 \times 10^{-5}$ |

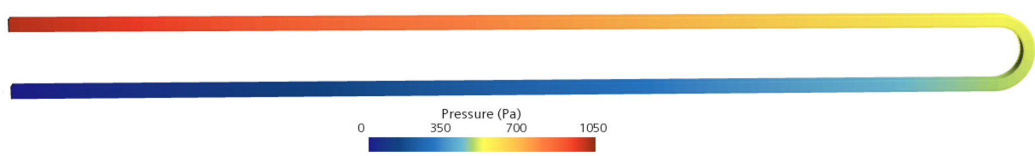


Figure S4: Pressure field within the microchannel obtained from numerical simulation for air flow at 1 ml/min.

## 4. Calibration Repeatability Test

To rigorously test the pressure sensor for its robustness and potential hysteresis, a test calibration was also performed for 4 consecutive runs using a separate sensor fabricated in the same way, where the applied pressure was varied following a pattern of 0 kPa – 2.4 kPa – 0 kPa – 2.4 kPa – 0 kPa at a step of 0.2 kPa. Essentially, the applied pressure was first increased from 0 kPa to 2.4 kPa at a step of 0.2 kPa (*i.e.*, Run 1), following which the pressure was gradually decreased all the way to 0 kPa (*i.e.*, Run 2). The entire process was then immediately repeated to get Run 3 and Run 4. As shown in Figure S5, the data from all 4 runs agrees very well, with a maximum RMSD of 0.042 kPa (1.75% of the calibrated range) between any two runs, suggesting a good repeatability and negligible hysteresis of the pressure sensor in the calibrated range.

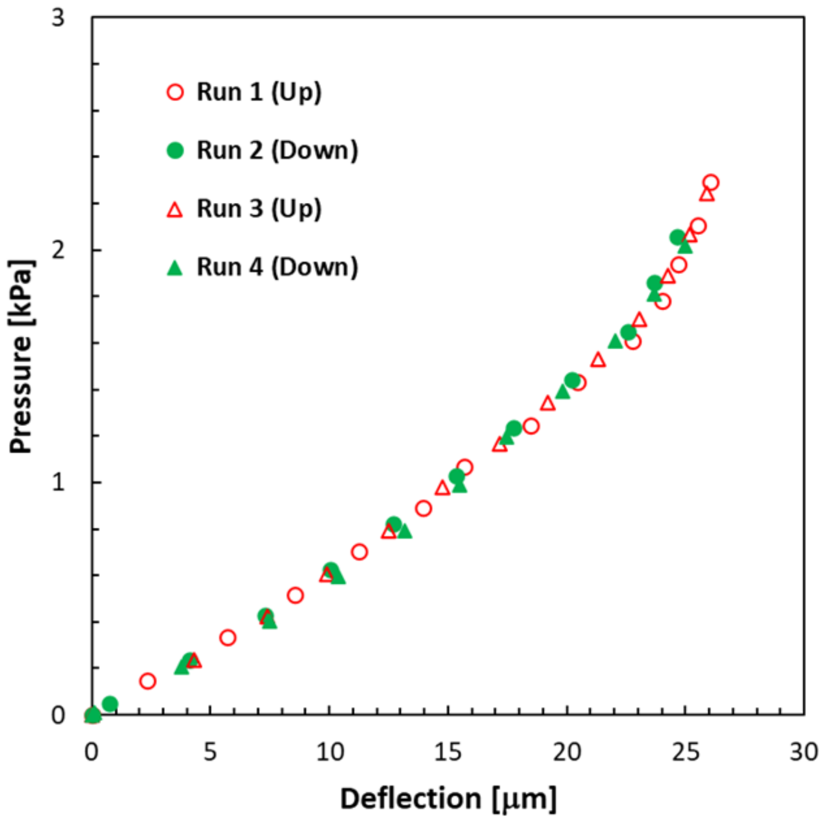


Figure S5: Repeatability test of the pressure calibration. To perform the test, the applied pressure was varied following the pattern of 0 kPa – 2.4 kPa – 0 kPa – 2.4 kPa – 0 kPa at a step of 0.2 kPa. The maximum root mean square deviation between any two runs is 0.042 kPa (1.75%), suggesting a good repeatability and negligible hysteresis of the pressure sensor.